



**HAL**  
open science

## Assessing the effects of $\beta$ -triketone herbicides on HPPD from environmental bacteria using a combination of in silico and microbiological approaches

Clémence Thiour-Mauprivez, Franck Emmanuel Dayan, Hugo Terol, Marion Devers, Christophe Calvayrac, Fabrice Martin-Laurent, Lise Barthelmebs

### ► To cite this version:

Clémence Thiour-Mauprivez, Franck Emmanuel Dayan, Hugo Terol, Marion Devers, Christophe Calvayrac, et al.. Assessing the effects of  $\beta$ -triketone herbicides on HPPD from environmental bacteria using a combination of in silico and microbiological approaches. *Environmental Science and Pollution Research*, 2023, 30, pp.9932-9944. 10.1007/s11356-022-22801-7 . hal-03927140

**HAL Id: hal-03927140**

**<https://hal.science/hal-03927140>**

Submitted on 17 Jan 2023

**HAL** is a multi-disciplinary open access archive for the deposit and dissemination of scientific research documents, whether they are published or not. The documents may come from teaching and research institutions in France or abroad, or from public or private research centers.

L'archive ouverte pluridisciplinaire **HAL**, est destinée au dépôt et à la diffusion de documents scientifiques de niveau recherche, publiés ou non, émanant des établissements d'enseignement et de recherche français ou étrangers, des laboratoires publics ou privés.

1 **Assessing the effects of  $\beta$ -triketone herbicides on HPPD from environmental bacteria using a**  
2 **combination of *in silico* and microbiological approaches**

3 **THIOUR-MAUPRIVEZ Clémence<sup>1,2</sup>, DAYAN Franck Emmanuel<sup>3</sup>, TEROL Hugo<sup>1</sup>, DEVERS-**  
4 **LAMRANI Marion<sup>2</sup>, CALVAYRAC Christophe<sup>1</sup>, MARTIN-LAURENT Fabrice<sup>2</sup>,**  
5 **BARTHELMEBS Lise<sup>1</sup>**

6 <sup>1</sup>Univ. Perpignan Via Domitia, Biocapteurs-Analyses-Environnement, 66860 Perpignan, France;  
7 Laboratoire de Biodiversité et Biotechnologies Microbiennes, USR 3579 Sorbonne Universités (UPMC)  
8 Paris 6 et CNRS Observatoire Océanologique, 66650 Banyuls-sur-Mer, France.

9 <sup>2</sup>Agroécologie, INRAE, Institut Agro, Univ. Bourgogne, Univ. Bourgogne Franche-Comté, F-21000  
10 Dijon, France

11 <sup>3</sup>Agricultural Biology Department, Colorado State University, Fort Collins CO 80523, USA

12 \*Corresponding author: barthelm@univ-perp.fr; +33468662256; +33468662223

13  
14 **Acknowledgements:** The authors kindly thank Marie Frenco and Tiffany Ferrer for their experimental  
15 work. The authors kindly thank Aleixei Sokorine for providing the *B. cereus* ATCC14579 strain, Charles  
16 Turick for the *S. oneidensis* MR-1 strain, Maria Esperanza Martinez Romero for *R. etli* CFN42, Fergual  
17 O’Gara for *P. fluorescens* F113 and Sylvie Mazurier for both *P. fluorescens* CTR1015 and NEM419.

18  
19  
20  
21  
22  
23  
24  
25  
26  
27  
28  
29  
30  
31  
32  
33  
34  
35

36 **Abstract:**

37 4-hydroxyphenylpyruvate dioxygenase (HPPD) is the molecular target of  $\beta$ -triketone herbicides in  
38 plants. This enzyme, involved in the tyrosine pathway, is also present in a wide range of living  
39 organisms, including microorganisms. Previous studies, focusing on a few strains and using high  
40 herbicide concentrations, showed that  $\beta$ -triketones are able to inhibit microbial HPPD. Here, we  
41 measured the effect of agronomical doses of  $\beta$ -triketone herbicides on soil bacterial strains. The HPPD  
42 activity of six bacterial strains was tested with  $1\times$  or  $10\times$  the recommended field dose of the herbicide  
43 sulcotrione. The selected strains were tested with  $0.01\times$  to  $15\times$  the recommended field dose of  
44 sulcotrione, mesotrione and tembotrione. Molecular docking was also used to measure and model the  
45 binding mode of the three herbicides with the different bacterial HPPD. Our results show that responses  
46 to herbicides are strain-dependent with *Pseudomonas fluorescens* F113 HPPD activity not inhibited by  
47 any of the herbicide tested; when all three  $\beta$ -triketone herbicides inhibited HPPD in *Bacillus cereus*  
48 ATCC14579 and *Shewanella oneidensis* MR-1. These responses are also molecule-dependent with  
49 tembotrione harboring the strongest inhibitory effect. Molecular docking also reveals different binding  
50 potentials. This is the first time that the inhibitory effect of  $\beta$ -triketone herbicides is tested on  
51 environmental strains at agronomical doses, showing a potential effect of these molecules on the HPPD  
52 enzymatic activity of non-target microorganisms.

53

54

55

56

57

58

59

60

61

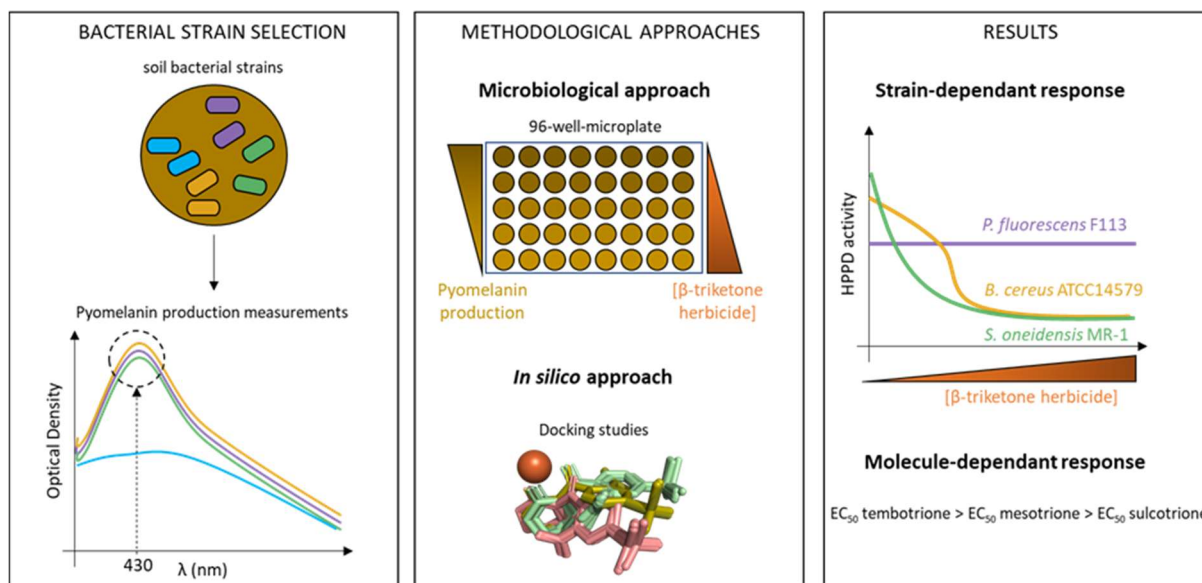
62

63

64

65

66 **Graphical abstract:**



67

68 **Keywords:** pyomelanin; 4-hydroxyphenylpyruvate dioxygenase; soil bacteria; β-triketone herbicides;  
 69 tembotrione; molecular docking.

70 **Introduction**

71 Herbicides account for 60% of the volume of all plant protection products applied worldwide [1], and  
 72 for 30% in the European Union Member States (EU Eurostats). Following atrazine ban in Europe in  
 73 2003, β-triketones herbicides have been commonly used as pre- and post-emergent selective compounds  
 74 and are among the top five most used herbicides on maize crops. β-triketones herbicides are synthesized  
 75 based on the structure of leptospermone, a natural phytotoxin produced by the Californian bottlebrush  
 76 plant, *Callistemon citrinus* [2]. Sulcotrione (2-(2-chloro-4-methylsulfonylbenzoyl)cyclohexane-1,3-  
 77 dione) was the first β-triketone herbicide commercialized [3], followed by mesotrione (2-[4-  
 78 (methylsulfonyl)-2-nitrobenzoyl]cyclohexane-1,3-dione) and, more recently, by tembotrione (2-[2-  
 79 chloro-4-methylsulfonyl-3-(2,2,2-trifluoroethoxymethyl)benzoyl]cyclohexane-1,3-dione) [4] (**Table**  
 80 **1**).

81 Plant 4-hydroxyphenylpyruvate dioxygenase (HPPD, EC 1.13.11.27) is the biochemical target of β-  
 82 triketones herbicides. This enzyme is a non-heme iron enzyme involved in the second reaction of the  
 83 tyrosine catabolism pathway by converting 4-hydroxyphenylpyruvate (HPP) in homogentisate (HGA)  
 84 *via* oxidative decarboxylation, aromatic ring hydroxylation and carboxymethyl group rearrangement [5].  
 85 HGA is a key precursor of α-tocopherol and plastoquinone, that acts as an essential cofactor for phytoene  
 86 desaturase, allowing plants to produce carotenoids required to protect them from light and free radicals  
 87 [6].

88 HPPD is ubiquitous in almost all living organisms [7]. In non-photosynthetic organisms, including  
89 humans, HPPD is also involved in tyrosine degradation, leading to HGA synthesis, the latter is involved  
90 in the synthesis pathway of fumarate, one of the intermediates of the Krebs cycle, and acetoacetate,  
91 involved in lipid biosynthesis [8].

92 In some microorganisms, HPPD activity is linked to pyomelanin production, a pigment accumulating  
93 following oxidation and polymerization of HGA. This brown pigment is easily observable on culture  
94 media supplemented with L-tyrosine, and its production has been described in various microbial species  
95 such as fungi and yeasts [9–12] and in numerous bacterial species such as *Legionella pneumophila*,  
96 *Shewanella oneidensis*, *Streptomyces avermitilis*, *Burkholderia cenocepacia*, *Bacillus thuringiensis*,  
97 *Alteromonas stellipolaris*, *Rubrivivax benzoatilyticus*, *Klebsiella pneumoniae*, *Alcaligenes faecalis*,  
98 *Enterobacter* sp. and *Vibrio angillarum* [13–21]. Some of these studies report either a protective role  
99 of pyomelanin against environmental stresses, such as reactive oxygen species for the soil-borne plant  
100 pathogen *Ralstonia solanacearum* [22], light for *L. pneumophila* [23], ultraviolet irradiation for the  
101 marine bacteria *Vibrio splendidus* [24], or a modification in virulence for pathogenic bacteria [19],  
102 highlighting the importance of deciphering HPPD function in microbes.

103 Nonetheless, microbial HPPD structure and  $\beta$ -triketone herbicide binding mode are only described in  
104 two microorganisms : *Pseudomonas fluorescens* F113 (also called *Pseudomonas kilonensis* F113 [25])  
105 and *Streptomyces avermitilis* [14,26]. Studies on binding modes of  $\beta$ -triketones were mainly performed  
106 on HPPD plant models such as *Arabidopsis thaliana* [5,27,28]. Most inhibition studies are performed  
107 on recombinant plants or bacterial HPPD cloned and expressed in *Escherichia coli* strains [29–31]. Only  
108 a few studies take an interest in deciphering the potential inhibition of soil microbial HPPD by  $\beta$ -  
109 triketone herbicides under agronomical conditions [32]. Also, the effect of  $\beta$ -triketone herbicides on  
110 microbial pigmentation production has been tested only with few pure strains and always using high  
111 herbicide concentration (from 12 to 200 $\times$  the recommended field dose (RfD)) [16,21,33].

112 As the use of  $\beta$ -triketone herbicides on crops continues to expand, it is important to assess their effect  
113 on “non-target organisms” [34], and especially on the HPPD activity of soil microbiota. We could  
114 wonder if the protective role of pyomelanin production against environmental stresses observed in some  
115 bacterial species, could be modified by the application of  $\beta$ -triketone herbicides on crops. Such an effect  
116 could affect the balance of soil microbiota and alter, for example, microbial populations playing a key  
117 role in plant growth, such as Plant Growth Promoting Rhizobacteria (PGPR), and consequently could  
118 have an impact on soil ecosystem services.

119 The aim of this study is to decipher the possible impacts of three triketone molecules on the HPPD  
120 enzymatic activities of different bacterial strains belonging to various genera. Six environmental  
121 bacterial strains were selected and tested for their pyomelanin production. Strains were exposed to 1 $\times$

122 or 10× RfD of sulcotrione. Three strains, selected according to their different sensitivities to sulcotrione,  
123 were then exposed, in a whole-cell assay, to increasing doses of three β-triketone herbicides, namely  
124 sulcotrione, mesotrione and tembotrione. As the calculated EC<sub>50</sub> (half-maximum Effective  
125 Concentration) varied depending the strain and the molecule considered, *in silico* molecular docking  
126 was performed to document the binding mode of β-triketones with bacterial HPPD and to explain, at a  
127 molecular level, the differences observed in the whole-cell assay when working at a population level.

## 128 **Material and methods**

### 129 **Bacterial strains and culture conditions**

130 *B. cereus* ATCC14579, *P. fluorescens* F113, *P. fluorescens* CTR1015 and *P. fluorescens* NEM419 were  
131 cultured in a Lysogenic Broth (LB: 10 g/l tryptone; 5 g/l yeast extract; 10 g/l NaCl). *S. oneidensis* MR-  
132 1 was grown in a Tryptic Soy Broth (TSB: 17 g/l tryptone; 3 g/l soy; 5 g/l NaCl; 2.5 g/l K<sub>2</sub>HPO<sub>4</sub>; 2.5 g/l  
133 glucose) and *R. etli* CFN42 in Tryptone Yeast extract media supplemented with CaCl<sub>2</sub> (TY+CaCl<sub>2</sub>: 5  
134 g/l tryptone; 3 g/l yeast extract; 0.9 g/l CaCl<sub>2</sub>×2H<sub>2</sub>O; pH=6.8).

### 135 **Pyomelanin production**

136 In order to test their ability to produce pyomelanin, each of the six bacterial strains were grown in their  
137 appropriate culture medium supplemented with 0.9 g/l of tyrosine at 24 °C with constant shaking at 120  
138 rpm. Samples of each culture were collected at T0, 48 h, 72 h, and a last point between 6 to 10 days  
139 depending of the strain, and centrifugated at 5,000 rpm for 10 min. The absorbance spectra of cell-free  
140 supernatant were recorded in a UV-Vis spectrophotometer in the range of 250 to 600 nm, as soluble  
141 pyomelanin can be quantified at different wavelengths, ranging from 400 to 430 nm [18,21,22,29,35].  
142 The *E. coli* BL21 strain, known as a non-producing pyomelanin strain, was added to this experiment as  
143 negative control, and the *E. coli* BL21 HPPD, modified to produce pyomelanin, as the positive control  
144 [29].

### 145 **Bacterial resting cells preparation**

146 Resting cells were prepared for each of the six strains in Phosphate Buffer (PB) in order to work at  
147 constant biomass, in a unique solution, whatever the strain. Each bacterial strain was grown overnight  
148 at 28°C and 110 rpm in its appropriate culture medium. Overnight cultures were diluted and incubated  
149 in a new fresh appropriate medium during three to eight-hour according to its growth capacity, to reach  
150 the exponential phase of growth. Then, cells were harvested by centrifugation for 5 min at 5,000 rpm,

151 washed twice in 20 mM PB, and then resuspended in a volume of PB calculated to have an OD<sub>600</sub> of 3.  
152 In this way, biomass was similar in all the resting cells.

### 153 **Colorimetric method for HPPD activity monitoring using whole-cell assay in a 96-well multiplate** 154 **format**

155 To assess the HPPD activity of the six selected strains, a colorimetric test in a 96-well multiplate format  
156 was developed. 96-well-microplates were all filled with 50 µL of resting cells, and completed with 125  
157 µL of L-Tyrosine 1.8 g/l (pH 9), and with 75 µL of herbicide solutions diluted in PB for the assays (A)  
158 or with 75 µL of PB for the positive control (PC). For the negative control (NC), only 200 µL of PB  
159 were added to the resting cells. Herbicide concentrations ranged from 0.05 to 15 times of the RfD for  
160 each molecule tested; corresponding to: 0.23 to 67.5 µM for sulcotrione; 0.22 to 66 µM for mesotrione  
161 and 0.17 to 52.5 µM for tembotrione. All herbicides solutions were prepared in PB. All controls and  
162 assays were performed in triplicate. Microplates were covered with a Breathseal sealer (Greiner Bio-  
163 One™, Germany) and incubated at 28°C and 110 rpm. After 48 hours of incubation, OD<sub>430</sub>, and OD<sub>600</sub>  
164 were measured using an Epoch 2 Microplate Spectrophotometer (Greiner Bio-One™, Germany).  
165 Pyomelanin detection was measured at OD<sub>430</sub> rather than OD<sub>400</sub> because of a better signal observed at  
166 this wavelength due to the resting cell mode done in PB. PB solely had the same absorbance as empty  
167 wells and was not included to our controls. In the second experiment, microplates were first centrifuged  
168 at 6000 rpm for 6 minutes and OD<sub>430</sub> of the supernatant was measured.

169 For each triplicate, normalized OD<sub>430</sub> (OD<sub>430N</sub>) was calculated according to:

$$170 \text{OD}_{430N} = \text{OD}_{430A} \text{ (or } \text{OD}_{430PC}) - \text{OD}_{430NC}$$

171 where OD<sub>430A</sub> is the mean OD<sub>430</sub> measured at various concentrations of herbicide, OD<sub>430PC</sub> is the mean  
172 OD<sub>430</sub> measured at 0 µM of herbicide (i.e. PC) and OD<sub>430NC</sub> is the mean OD<sub>430</sub> measured for the NC.

173 The enzymatic activity percentage, Act. %, was calculated according to the equation:

$$174 \text{Act. \%} = \left( \frac{\text{OD}_{430A}}{\text{OD}_{430PC}} \right) \times 100$$

### 175 **Dose-response curves**

176 For each herbicide tested, EC<sub>50</sub> was calculated using the “*drc*” package in R [36]. A three-parameter  
177 log-logistic function with lower limit 0 was applied to our datasets, corresponding to this equation:

178 
$$f(x) = 0 + \frac{d - 0}{1 + \exp(b(\log(x) - \log(e)))}$$

179 where b, d and e are estimated by the model with a p<0.05.

## 180 **In silico analysis**

181 Protein sequences were retrieved from GenBank (<https://www.ncbi.nlm.nih.gov/genbank/>) with  
182 WP\_000810922.1 corresponding to the accession number of *B. cereus* ATCC14579 HPPD sequence  
183 and WP\_011072057.1, WP\_011425038.1 and WP\_014347821.1 corresponding to the HPPD sequences  
184 of *S. oneidensis* MR-1, *R. etli* CFN42 and *P. fluorescens* F113 respectfully. The protein sequences of  
185 both *P. fluorescens* CTR1015 and *P. fluorescens* NEM419 are not available yet. Protein sequences of  
186 *L. pneumophila* (WP\_011216180.1), *P. aeruginosa* (PWU35210.1), *A. salmonicida*  
187 (WP\_059112190.1), *V. parahaemolyticus* (WP\_057619320.1) and *V. anguillarum* (QEH62709.1) were  
188 also added to the analysis. Sequences were aligned using ClustalW [37].

## 189 *Homology modelling*

190 Homology models of each of the HPPDs were obtained using the multiple alignment function of  
191 Modeller version 9.22 [38,39], including the crystal structures of HPPD from *Streptomyces avermitilis*  
192 and from *Arabidopsis thaliana* (1t47 and 5yy6, respectively) [14,40]. The crystal structure of *A. thaliana*  
193 was included because it incorporates the conformational change known to occur upon binding of the  
194 inhibitors. Preliminary models with the lowest DOPE scores were selected for further refinement using  
195 GROMACS (version 2018.3) [41,42]. The structures were relaxed to correct for steric clashes or  
196 inappropriate geometries prior to molecular dynamics simulation. The final topology of the homology  
197 models were evaluated using MolProbity [43,44].

## 198 *Docking of herbicides*

199 The structures of mesotrione and tembotrione were downloaded as sdf files from PubChem  
200 ([pubchem.ncbi.nlm.nih.gov](http://pubchem.ncbi.nlm.nih.gov)), edited with Spartan18 (Wavefunction Inc., Irvine CA 92612) to include  
201 delocalized -1 charges over two of the three keto groups, and saved as saved as pdb files. The structures  
202 were converted to Autodock compatible pdbqt format using AutoDockTools (version 1.5.6). These  
203 herbicides were docked to the catalytic domain of HPPD using Autodock4 [45,46], using the iron metal  
204 dication (with a +0.6 partial charge) as an anchor [44] and the following conserved residues (T164,  
205 S202, P215, N217, Q240, L295, F312, F321, L341, F333, N337, F338). The binding energy of the  
206 herbicides on the bacterial HPPD models were obtained from the dock.dlg file. Proteins and ligand



207 interactions were visualized using PyMOL (The PyMOL Molecular Graphics System, Version 2.0  
208 Schrödinger, LLC) [47].

## 209 **Results and discussion**

### 210 **Pyomelanin production in the six bacterial strains**

211 In order to study the potential effect of  $\beta$ -triketones on microbial HPPD activity, six environmental  
212 bacterial strains were selected: *Pseudomonas fluorescens* F113, as the HPPD study model [26], two *P.*  
213 *fluorescens* strains CTR1015 and NEM419 as PGPR bacteria models isolated from soil [48,49],  
214 *Rhizobium etli* strain CFN42 as a symbiotic bacteria model [50], the well-studied pyomelanin producer  
215 *Shewanella oneidensis* MR-1 [22] and *Bacillus cereus* ATCC14579 the only Gram-positive bacterium  
216 of this study [51].

217 A first experiment was performed to validate that these six bacterial strains produce pyomelanin. As  
218 previously described, soluble pyomelanin can be quantified measuring absorbance at different  
219 wavelengths, ranging from 400 to 430 nm [16,18,21,22,29]. Spectrophotometric analysis of cell-free  
220 supernatants of the six strains showed a significant increase of OD<sub>400</sub> between the different sampling  
221 time, similar to what observed for *P. fluorescens* F113 (**Supplementary Information 1a**). Final OD<sub>400</sub>  
222 were reported for the six tested strains, and for the two controls, validating the pyomelanin production  
223 for the studied bacterial strains (**Supplementary Information 1b**).

### 224 **Development of a multiplate colorimetric whole-cell assay for HPPD activity analysis**

225 To assess the HPPD activity of the six selected strains, a colorimetric test in a 96-well multiplate format  
226 was developed. Resting cells were prepared for each of the six strains in PB and added to the assay in  
227 order to work at constant biomass, in a unique solution whatever the strain. Then, OD<sub>430</sub>, characterizing  
228 the melanin-like pigment, and thus, reflecting the HPPD activity [18,29] was, for each strain, directly  
229 measured in each well containing bacterial resting cells, PB and tyrosine. *P. fluorescens* F113 HPPD  
230 expressed the highest production of pyomelanin pigment with an OD<sub>430N</sub> of  $1.43 \pm 0.11$ , followed by *P.*  
231 *fluorescens* CTR1015 and NEM419 with OD<sub>430N</sub> of  $0.86 \pm 0.01$  and  $0.74 \pm 0.02$  respectively, and then  
232 *S. oneidensis* MR-1, *B. cereus* ATCC14579 and *R. etli* CFN42 with OD<sub>430N</sub> of  $0.70 \pm 0.12$ ;  $0.66 \pm 0.07$   
233 and  $0.55 \pm 0.03$  respectively (**Supplementary Information 2**). These results were similar to those  
234 obtained in the first experiment, validating the miniaturization of the assay, and the pigmentation  
235 measurement in PB.

### 236 **Studying the effect of $\beta$ -triketones on HPPD activity using the colorimetric whole-cell assay**

237 The resting cells of the six bacterial strains of our study were exposed or not to 1×RfD or 10×RfD of  
238 sulcotrione. The HPPD enzymatic activity percentage (Act. %) was calculated for each strain and is  
239 depicted in **Figure 1**. In *B. cereus* ATCC14579, *S. oneidensis* MR-1 and *P. fluorescens* CTR1015,  
240 HPPD activity clearly decreased with increasing doses of sulcotrione, with a decrease of, at least, 31 %  
241 at 1×RfD, and of, at least, 74 % at 10×RfD. In *R. etli* CFN42, HPPD activity decreased of 15% at  
242 1×RfD and 12% at 10×RfD. In *Pseudomonas* NEM 419 enzymatic activity remained unchanged at  
243 1×RfD but decreased of 50% at 10×RfD. On the contrary, HPPD activity of *P. fluorescens* F113  
244 slightly decreased in response to sulcotrione exposure but not significantly compared to the control.  
245 There is indeed a strain-dependant response to sulcotrione, even within strains belonging to the same  
246 genus. To characterize more accurately the inhibition of bacterial HPPD activity in response to  
247 sulcotrione, two bacterial strains were exposed to increasing doses of this herbicide, more finely between  
248 0 and 10×RfD. *P. fluorescens* F113, in which the HPPD is well described and which is known to have  
249 an ecological role in rhizosphere, was considered in these experiments [25,26]. As *P. fluorescens* F113  
250 HPPD activity does not seem to be affected by sulcotrione, we also exposed *S. oneidensis* MR-1 to this  
251 herbicide, a strain in which the HPPD activity was well-documented [16]. The obtained results  
252 confirmed our previous observations: *P. fluorescens* F113 OD<sub>430N</sub> appeared constant even with 10×RfD  
253 of sulcotrione (**Figure 2.A**) whereas the one of *S. oneidensis* MR-1 was drastically decreasing  
254 proportionally to the RfD of sulcotrione, losing around 50% of HPPD activity from 2×RfD of  
255 sulcotrione (**Figure 2.B**). This first assay informed us about the existence of tolerant HPPD activities,  
256 such as the one of *P. fluorescens* F113, and sensitive one, such as the one of *S. oneidensis* MR-1. This  
257 phenomenon has already been reported for bacterial strains carrying acetohydroxyacid synthase  
258 (AHAS), the target enzyme of the sulfonylurea herbicides (SN). Enterobacteriaceae, carrying AHAS  
259 isoform 1 are tolerant to SN, whereas other bacteria carrying isoform 2 or 3 are sensitive to those  
260 herbicides [32,52]. Concerning *P. fluorescens* F113, one may hypothesize either such a difference  
261 between several bacterial HPPD isoforms, or a possible detoxification phenomenon supporting  
262 resistance to β-triketones specific to this bacterial strain. In this latter case, detoxification could be  
263 achieved by the transformation of the active compound. Although *P. putida* 1OP is known to degrade  
264 sulcotrione and used it as a source of carbon [53], the transformation of β-triketones by *P. fluorescens*  
265 F113 has not yet been described. Detoxification can also be achieved by efflux pumps that are pumping  
266 herbicides out of the cell. As an example, a putative major facilitator superfamily (MFS) transporter  
267 encoded by the *yhhS* gene conferred resistance in an *E. coli* strain to glyphosate [54]. Efflux pumps are  
268 commonly described in Gram-negative and especially in *P. aeruginosa* where they impart resistance to  
269 antibiotics [55,56]. Other studies have tested the HPPD activity of *P. aeruginosa* strains in presence of  
270 NTBC, a β-triketone used in human medicine, and inhibitory effects are observed at high doses of the  
271 inhibitor. For the DKN343 and 1111 isolates, NTBC (up to 900 μM) showed no inhibitory effects on  
272 HPPD activity and in the PAO1 mutant, *P. aeruginosa* *hmgA::tn*, 300 μM of NTBC are required to  
273 inhibit the enzyme activity [57]. The same authors showed that the expression of the *MexAB-OprM*

274 efflux pump is required for resistance to NTBC in DKN343 [58]. This efflux pump is known to pump  
275 out a broad range of antibiotics, detergents or organic solvents [59]. We can then hypothesize that a  
276 similar efflux pump can allow  $\beta$ -triketone such as sulcotrione, to be pumped out by *P. fluorescens* F113.  
277 Anyhow, further studies reporting a possible expression of genes encoding efflux pumps in parallel with  
278 an exposition to sulcotrione could be needed to reinforce this hypothesis.

### 279 Designing dose-response curves on three bacterial models

280 In order to refine our results, we decided to expose to other  $\beta$ -triketone herbicides three of the six  
281 bacterial strains: a Gram-negative harbouring a sensitive HPPD activity (*S. oneidensis* MR-1), a tolerant  
282 one (*P. fluorescens* F113), and the only Gram-positive (*B. cereus* ATCC14579). Using the colorimetric  
283 whole-cell assay, resting cells of *S. oneidensis* MR-1, *B. cereus* ATCC14579 and *P. fluorescens* F113  
284 were exposed to increasing doses of sulcotrione, mesotrione and tembotrione. The pre-screening at high  
285 doses of herbicides allowed us to select specific inhibitory concentrations ranging from  $0\times$  to  $10\times$  RfD  
286 for sulcotrione (**Figure 3.A**),  $0\times$  to  $0.5\times$  RfD for mesotrione (**Figure 3.B**) and  $0\times$  to  $0.07\times$  RfD for  
287 tembotrione (**Figure 3.C**). As previously showed with sulcotrione, the HPPD activity of *P. fluorescens*  
288 F113 is not inhibited by any of the three  $\beta$ -triketones tested (**Figure 3.A, 3.B and 3.C**) even at high  
289 doses, up to  $15\times$  RfD (data not shown). At these concentrations, a clear dose-dependent response was  
290 observed in *B. cereus* ATCC14579 and *S. oneidensis* MR-1 which allowed us to calculate  $EC_{50}$  for the  
291 different herbicides. Tembotrione appears to have the strongest inhibiting effect on the HPPD activity  
292 of both bacteria. Indeed,  $EC_{50}$  are not even calculable due to a too rapid decrease of HPPD activity.  
293 However, we can assume that, for both *B. cereus* ATCC14579 and *S. oneidensis* MR-1,  $EC_{50}$  is below  
294  $0.02\times$  RfD of tembotrione, corresponding to  $0.07\ \mu\text{M}$ , and that tembotrione has a slightly higher effect  
295 on the HPPD activity of *S. oneidensis* MR-1. Similarly, mesotrione has a lower effect on the HPPD  
296 activity of *B. cereus* ATCC14579 with an  $EC_{50}$  of  $2.2 \pm 0.3\ \mu\text{M}$  than on the one of *S. oneidensis* MR-1  
297 for which the  $EC_{50}$  cannot be calculated because a too rapid decrease of its HPPD activity but can be  
298 easily graphically estimated below  $0.2\times$  RfD of mesotrione, being  $0.88\ \mu\text{M}$ . Sulcotrione appears to be  
299 the active compound with the lowest effect whatever the strain considered with an  $EC_{50}$  of  $8.5 \pm 3.3\ \mu\text{M}$   
300 in *B. cereus* ATCC14579 and  $8.8 \pm 2.8\ \mu\text{M}$  in *S. oneidensis* MR-1. This experiment confirmed our  
301 previous results with a strain-dependant response but also highlights a molecule-dependant response.  
302 Indeed,  $\beta$ -triketones were ranked as follows from the highest to the lowest inhibitory effect: tembotrione,  
303 mesotrione and sulcotrione. Tembotrione appears then to have the lowest  $EC_{50}$  in both *B. cereus*  
304 ATCC14579 and *S. oneidensis* MR-1. This molecule was shown to be more toxic on the earthworm  
305 *Dendrobaena veneta* than glyphosate and nicosulfuron [60]. Even though the cited study did not  
306 compare tembotrione to other  $\beta$ -triketones, it provides insights in its potential toxicity. When cloned in  
307 *E. coli*, the topramezone-resistant HPPD of the bacterium *Sphingobium* sp. TPM-19 exhibits a higher  
308 resistance to mesotrione ( $EC_{50}$  of  $4.2\ \mu\text{M}$ ) compared to tembotrione ( $EC_{50}$  of  $2.5\ \mu\text{M}$ ) [31] suggesting

309 that, as observed in our study, tembotrione is more active than mesotrione on HPPD activity even for  
310 resistant HPPDs. This higher activity might be due to the fluorinated tail (-O-CH<sub>2</sub>-CF<sub>3</sub>) which increases  
311 its lipophilicity and favors the passage of hydrophilic and lipophilic barriers [61]. However, tembotrione  
312 physico-chemical properties such as solubility or pKa do not explain its little or no effect on the HPPD  
313 enzymatic activity of *P. fluorescens* F113. One can notice that the *MexAB-OprM* efflux pump previously  
314 cited is not yet described neither in *B. cereus* ATCC14579 nor in *S. oneidensis* MR-1, suggesting that  
315 these bacteria cannot extrude tembotrione once it has entered the cell. Regarding a possible  
316 biodegradation mechanism of tembotrione, the trifluoromethyl group added to this compound could  
317 make difficult its biodegradation. Moreover, it is known that, in soils, half-life time (DT<sub>50</sub>) of  
318 sulcotrione, mesotrione and tembotrione are comprised between 3.2 and 144 days depending on the soil  
319 tested [61]. A possible abiotic or biotic degradation in our culture conditions is, then, quite unlikely.  
320 Taken together, these hypotheses can explain the fact that tembotrione harbors a higher inhibitory effect  
321 on the HPPD activities of certain bacteria than sulcotrione does.

322 Beyond the cellular level, one can imagine that such strain- and molecule-dependent responses may also  
323 be due to molecular changes in the studied HPPD. As it is the case in plants where maize harbors a  
324 resistant HPPD [62], bacteria could also harbor HPPD with different sensitivities to  $\beta$ -triketones.

### 325 ***In silico* HPPD sequences analysis**

326 We then conducted *in silico* analysis in order to identify possible differences in the HPPD sequences of  
327 the tested strains and, following that, molecular docking was led to identify different binding responses.  
328 HPPD protein sequences of the three bacteria previously studied were aligned (**Supplementary**  
329 **Information 3**), together with the HPPD of *R. etli* CFN42, which was available online and was part of  
330 our first experiment, and five others HPPD sequences from different bacteria strains, whose pyomelanin  
331 production has been described [13,19,63,64]. Even though these nine sequences have relatively low  
332 similarity, ranging from 35.26 to 87.39%, they retain some highly conserved regions. Firstly, the  
333 catalytic domain, located in the C-terminus involves a triad consisting of one glutamate (E) and two  
334 histidine (H) residues. This triad is highly conserved in bacteria, plant and mammalian forms of HPPD,  
335 because these three residues coordinate the binding of a metal dication (either Fe or Co) involved in the  
336 catalytic function of HPPD [26,62] (**Figure 4A**), thus playing an essential role in enzyme function.  
337 Always in the C-terminal region, the motifs H-I/V/L/L-A and F-F/I/V/L-E, common across HPPD from  
338 different bacterium phyla are identified. They are typical from the active site of the enzyme and are  
339 conserved among 2506 bacterial protein sequences [65]. Additionally, the binding domain of the  
340 substrate HPP is a highly conserved area formed by mostly hydrophobic residues (T164, S202, P215,  
341 N217, Q240, L295, F312, F321, F333, N337, F338, L341 based on sequence of *P. fluorescens* HPPD)  
342 (**Figure 4C and Supplementary Information 3 and 4**). These 12 amino acids present almost 100% of

343 identity with just one exception for the HPPD sequence of *B. cereus* in the position 164, where a Valine  
344 replace Tyrosine. This binding domain plays an important role in positioning HPP in the proper position  
345 for the region specific hydroxylation reaction catalyzed by HPPD [66].  $\beta$ -triketone herbicides are known  
346 to interact at this interphase by forming a stable complex between two of their keto groups towards a  
347 bidentate association with the active-site metal ion by coordinate as well as this hydrophobic domain  
348 [14]. Amino acid sequence comparison of the bacterial HPPD revealed a highly conserved active site  
349 and could not explain the differences of inhibition previously observed between the different strains of  
350 our study when working on the whole-cell assay. Similar observations were done when HPPD sequence  
351 of maize, whose HPPD is naturally tolerant to  $\beta$ -triketone, was compared with other HPPD sequences  
352 from  $\beta$ -triketone sensible plants as *A. thaliana* [62].

353 To go further, molecular docking was then carried out with the HPPD from bacterial strains either  
354 sensitive or tolerant to  $\beta$ -triketone to explore the complex formed between bacterial enzyme and  
355 inhibitors.

#### 356 **Docking of sulcotrione, mesotrione and tembotrione to microbial HPPD**

357 The capacity of the three  $\beta$ -triketone compounds to fit within the substrate binding pocket of the  
358 microbial HPPD of *S. oneidensis* MR-1, *B. cereus* ATCC14579 and *P. fluorescens* F113 was estimated  
359 by the binding energy. This parameter was determined for each docking experiments as the average of  
360 the energy of the correct orientations between the herbicide and the ligand based on homology model of  
361 *P. fluorescens* F113. For example, the docking results obtained with mesotrione coordinated on the  
362 metal dication on homology model of *P. fluorescens* F113 generated 25 different poses. On these 25  
363 poses generated by the docking algorithm, 18 were in an orientation most similar to that observed with  
364 inhibitors co-crystallized with HPPD, 3 were in the less favourable pose and 4 in the least desirable  
365 orientation (**Supplementary Information 5**). Regardless of the poses, all docking resulted in proper  
366 interaction with the iron metal dication (**Supplementary Information 6**).

367 As we can observed, molecular docking revealed that sulcotrione, mesotrione and tembotrione are able  
368 to bind with HPPD of *B. cereus* ATCC14579, *S. oneidensis* MR-1 and *P. fluorescens* F113. Whatever  
369 the strain, docking results suggest that tembotrione and sulcotrione binds more tightly to the bacterial  
370 HPPDs tested than mesotrione. Regarding the number of docking achieving the preferred binding pose  
371 (similar to green pose in **Supplementary Information 6**), both sulcotrione and mesotrione docked  
372 correctly and more frequently than tembotrione. These latter observations do not correspond to the one  
373 obtained with whole-cell assay experiments where tembotrione had a higher inhibitory potential than  
374 sulcotrione and mesotrione whatever the strains. Interestingly, Moran *et al.*, suggest that HPPD inhibitor  
375 selectivity is based more on bioavailability of the molecule than on direct affinity for HPPD from a

376 specific organism [5]. This observation could explain the apparent discrepancy observed in the results  
377 between docking and whole-cell experiments.

378 Our results also showed that the binding force of the three tested  $\beta$ -triketones with the HPPD of *P.*  
379 *fluorescens* F113 is lower than the one of the two others strains, suggesting that these three compounds  
380 are less able to fit the substrate binding pocket of the HPPD of *P. fluorescens* F113 than that of the two  
381 others microbial HPPD. It is noteworthy that these docking predictions agree with the measurement  
382 done with our colorimetric whole-cell assay.

383 In fact, *P. fluorescens* F113, was tolerant to the tested  $\beta$ -triketones despite the fact that docking predicted  
384 that these active compounds can interact with the active site of its HPPD, even if this HPPD presents  
385 the lowest binding force of interaction. Therefore, this poor interaction with the HPPD enzyme of *P.*  
386 *fluorescens* F113 cannot only explained the  $\beta$ -triketone tolerance of this strain. Thus, *in silico* analysis  
387 is useful to understand and describe molecular interaction between the active compound and the target.  
388 However, it is not enough to fully predict the tolerance or the sensitivity of the bacterial HPPD to  $\beta$ -  
389 triketones because there are a range of other abiotic and biotic processes involved in the response  
390 bacterial cells to  $\beta$ -triketones. A new screening of bacterial strains having either tolerant or sensitive  
391 HPPD activity have to be done to gain more information and validate the docking results obtained with  
392 the three HPPD sequences of this study. Furthermore, additional experiments analysing the inhibitor  
393 binding kinetics on purified HPPDs from these microorganisms would yield important information  
394 regarding their affinity. Our docking provides insight on the  $K_{on}$  values of the herbicides, but it is well  
395 known that HPPD inhibitors bind very tightly to the target site [67]. Consequently, measuring the  $K_{off}$   
396 values might be even more insightful. Indeed, compounds with high  $K_{off}$  values (binding for a very  
397 short time) may not be very active. On the other hand, compounds with low  $K_{off}$  values (tight binding  
398 or irreversible inhibition) would potentially be more active [68]. However, this is beyond the scope of  
399 this paper.

## 400 **Conclusion**

401 At a molecular level, molecular docking reveals that tembotrione and sulcotrione appear to have a  
402 stronger binding force to the bacterial HPPD enzymes than mesotrione. However, *in silico* study shows  
403 that tembotrione binds less frequently than the two other molecules. At a cellular level, whole-cell assays  
404 show that inhibitory potential is also molecule dependent but with tembotrione on the top step of the  
405 podium. Such differences allow us to think that *in silico* and *in vivo* approaches complement each other.  
406 HPPD enzymatic activity inhibition also appears strain-dependent. At a molecular level, *P. fluorescens*  
407 F113 shows a lower binding force to herbicides than *B. cereus* ATCC14579 and *S. oneidensis* MR-1,  
408 confirming the observations made at the cellular level. By combining approaches at both cellular and

409 molecular levels, this is the first study that assesses the effect of agronomical doses of three  $\beta$ -triketone  
410 active compounds on the HPPD enzymatic activities of six environmental bacterial strains.

411 At the community level, a recent lab-to-field study demonstrates that, neither sulcotrione nor its  
412 formulated product, Decano<sup>®</sup>, has an effect on the abundance and the diversity of both total and *hppd*  
413 bacterial communities [32]. As we measure that tembotrione has a lower EC<sub>50</sub> than sulcotrione in some  
414 bacteria, conducting a lab-to-field experiment with tembotrione and one of its formulated products could  
415 be interesting. Actually, working at a lower biological level (*i.e.* whole-cell assay coupled with  
416 molecular docking) should be of interest, prior to conducting microcosm or field experiments, which  
417 are more difficult to set up.

418 Whole-cell assay developed in this study could be applied to other herbicides and pesticides that also  
419 target an enzyme harbored by non-target organisms and, more precisely, by microorganisms, like  
420 EPSPSynthase, targeted by Glyphosate or ALSynthase targeted by sulfonylurea herbicides [69], as there  
421 is a need to develop new tools for pesticide risk assessment on soil microorganisms [70,71].

## 422 **References**

- 423
- 424 1. Dayan FE (2019) Current Status and Future Prospects in Herbicide Discovery. *Plants Basel Switz*  
425 8.
  - 426 2. Beaudegnies R, Edmunds AJF, Fraser TEM, et al. (2009) Herbicidal 4-hydroxyphenylpyruvate  
427 dioxygenase inhibitors—A review of the triketone chemistry story from a Syngenta perspective.  
428 *Bioorg Med Chem* 17: 4134–4152.
  - 429 3. Schulz A, Ort O, Beyer P, et al. (1993) SC-0051, a 2-benzoyl-cyclohexane-1,3-dione bleaching  
430 herbicide, is a potent inhibitor of the enzyme p-hydroxyphenylpyruvate dioxygenase. *FEBS Lett*  
431 318: 162–166.
  - 432 4. Mitchell G, Bartlett DW, Fraser TE, et al. (2001) Mesotrione: a new selective herbicide for use in  
433 maize. *Pest Manag Sci* 57: 120–128.
  - 434 5. Moran GR (2005) 4-Hydroxyphenylpyruvate dioxygenase. *Arch Biochem Biophys* 433: 117–128.
  - 435 6. Norris SR, Barrette TR, DellaPenna D (1995) Genetic dissection of carotenoid synthesis in  
436 arabidopsis defines plastoquinone as an essential component of phytoene desaturation. *Plant*  
437 *Cell* 7: 2139–2149.
  - 438 7. Santucci A, Bernardini G, Braconi D, et al. (2017) 4-Hydroxyphenylpyruvate Dioxygenase and Its  
439 Inhibition in Plants and Animals: Small Molecules as Herbicides and Agents for the Treatment of  
440 Human Inherited Diseases. *J Med Chem* 60: 4101–4125.
  - 441 8. Dixon DP, Edwards R (2006) Enzymes of tyrosine catabolism in Arabidopsis thaliana. *Plant Sci*  
442 *Int J Exp Plant Biol* 171: 360–366.
  - 443 9. Schmalzer-Ripcke J, Sugareva V, Gebhardt P, et al. (2009) Production of pyomelanin, a second  
444 type of melanin, via the tyrosine degradation pathway in Aspergillus fumigatus. *Appl Environ*  
445 *Microbiol* 75: 493–503.
  - 446 10. Vasanthakumar A, DeAraujo A, Mazurek J, et al. (2015) Pyomelanin production in Penicillium  
447 chrysogenum is stimulated by L-tyrosine. *Microbiol Read Engl* 161: 1211–1218.

- 448 11. Almeida-Paes R, Almeida-Silva F, Pinto GCM, et al. (2018) L-tyrosine induces the production of a  
449 pyomelanin-like pigment by the parasitic yeast-form of *Histoplasma capsulatum*. *Med Mycol*  
450 56: 506–509.
- 451 12. Perez-Cuesta U, Aparicio-Fernandez L, Guruceaga X, et al. (2020) Melanin and pyomelanin in  
452 *Aspergillus fumigatus*: from its genetics to host interaction. *Int Microbiol Off J Span Soc*  
453 *Microbiol* 23: 55–63.
- 454 13. Steinert M, Flügel M, Schuppler M, et al. (2001) The Lly protein is essential for p-  
455 hydroxyphenylpyruvate dioxygenase activity in *Legionella pneumophila*. *FEMS Microbiol Lett*  
456 203: 41–47.
- 457 14. Brownlee JM, Johnson-Winters K, Harrison DHT, et al. (2004) Structure of the ferrous form of  
458 (4-hydroxyphenyl)pyruvate dioxygenase from *Streptomyces avermitilis* in complex with the  
459 therapeutic herbicide, NTBC. *Biochemistry* 43: 6370–6377.
- 460 15. Keith KE, Killip L, He P, et al. (2007) *Burkholderia cenocepacia* C5424 produces a pigment with  
461 antioxidant properties using a homogentisate intermediate. *J Bacteriol* 189: 9057–9065.
- 462 16. Turick CE, Beliaev AS, Zakrajsek BA, et al. (2009) The role of 4-hydroxyphenylpyruvate  
463 dioxygenase in enhancement of solid-phase electron transfer by *Shewanella oneidensis* MR-1.  
464 *FEMS Microbiol Ecol* 68: 223–225.
- 465 17. Zhu S, Lu Y, Xu X, et al. (2015) Isolation and identification of a gene encoding 4-  
466 hydroxyphenylpyruvate dioxygenase from the red-brown pigment-producing bacterium  
467 *Alteromonas stellipolaris* LMG 21856. *Folia Microbiol (Praha)* 60: 309–316.
- 468 18. Singh D, Kumar J, Kumar A (2018) Isolation of pyomelanin from bacteria and evidences showing  
469 its synthesis by 4-hydroxyphenylpyruvate dioxygenase enzyme encoded by hppD gene. *Int J Biol*  
470 *Macromol* 119: 864–873.
- 471 19. Batallones V, Fernandez J, Farthing B, et al. (2019) Disruption of hmgA by DNA Duplication is  
472 Responsible for Hyperpigmentation in a *Vibrio anguillarum* Strain. *Sci Rep* 9: 14589.
- 473 20. Tan T, Zhang X, Miao Z, et al. (2019) A single point mutation in hmgA leads to melanin  
474 accumulation in *Bacillus thuringiensis* BMB181. *Enzyme Microb Technol* 120: 91–97.
- 475 21. Mekala LP, Mohammed M, Chinthapati S, et al. (2019) Pyomelanin production: Insights into  
476 the incomplete aerobic l-phenylalanine catabolism of a photosynthetic bacterium, *Rubrivivax*  
477 *benzoatilyticus* JA2. *Int J Biol Macromol* 126: 755–764.
- 478 22. Ahmad S, Lee SY, Kong HG, et al. (2016) Genetic Determinants for Pyomelanin Production and  
479 Its Protective Effect against Oxidative Stress in *Ralstonia solanacearum*. *PLoS ONE* 11.
- 480 23. Steinert M, Engelhard H, Flügel M, et al. (1995) The Lly protein protects *Legionella pneumophila*  
481 from light but does not directly influence its intracellular survival in *Hartmannella vermiformis*.  
482 *Appl Environ Microbiol* 61: 2428–2430.
- 483 24. Liang W, Zhang W, Shao Y, et al. (2018) Dual functions of a 4-hydroxyphenylpyruvate  
484 dioxygenase for *Vibrio splendidus* survival and infection. *Microb Pathog* 120: 47–54.
- 485 25. Vacheron J, Desbrosses G, Renoud S, et al. (2018) Differential Contribution of Plant-Beneficial  
486 Functions from *Pseudomonas kilonensis* F113 to Root System Architecture Alterations in  
487 *Arabidopsis thaliana* and *Zea mays*. *Mol Plant-Microbe Interact MPMI* 31: 212–223.
- 488 26. Serre L, Sailland A, Sy D, et al. (1999) Crystal structure of *Pseudomonas fluorescens* 4-  
489 hydroxyphenylpyruvate dioxygenase: an enzyme involved in the tyrosine degradation pathway.  
490 *Struct Lond Engl* 1993 7: 977–988.
- 491 27. Meazza G, Scheffler BE, Tellez MR, et al. (2002) The inhibitory activity of natural products on  
492 plant p-hydroxyphenylpyruvate dioxygenase. *Phytochemistry* 60: 281–288.
- 493 28. Dayan FE, Singh N, McCurdy CR, et al. (2009) Beta-triketone inhibitors of plant p-  
494 hydroxyphenylpyruvate dioxygenase: modeling and comparative molecular field analysis of  
495 their interactions. *J Agric Food Chem* 57: 5194–5200.
- 496 29. Rocaboy-Faquet E, Noguer T, Romdhane S, et al. (2014) Novel bacterial bioassay for a high-  
497 throughput screening of 4-hydroxyphenylpyruvate dioxygenase inhibitors. *Appl Microbiol*  
498 *Biotechnol* 98: 7243–7252.

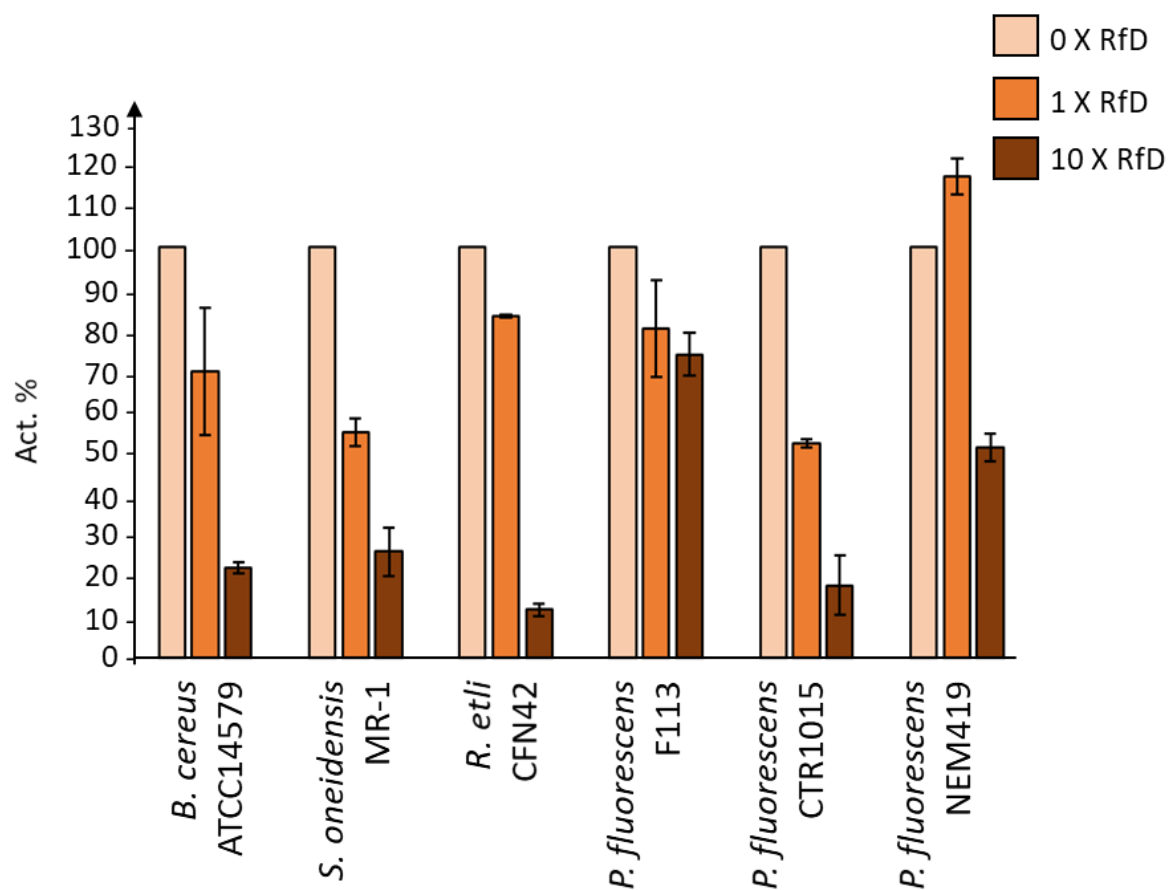


- 499 30. Neuckermans J, Mertens A, De Win D, et al. (2019) A robust bacterial assay for high-throughput  
500 screening of human 4-hydroxyphenylpyruvate dioxygenase inhibitors. *Sci Rep* 9: 14145.
- 501 31. Liu B, Peng Q, Sheng M, et al. (2020) Isolation and Characterization of a Topramezone-Resistant  
502 4-Hydroxyphenylpyruvate Dioxygenase from *Sphingobium* sp. TPM-19. *J Agric Food Chem* 68:  
503 1022–1029.
- 504 32. Thiour-Mauprivez C, Devers-Lamrani M, Bru D, et al. (2020) Assessing the effects of  $\beta$ -triketone  
505 herbicides on the soil bacterial and hppd communities: a lab-to-field experiment. *Front*  
506 *Microbiol* 11.
- 507 33. Almeida-Paes R, Frases S, Araújo G de S, et al. (2012) Biosynthesis and Functions of a Melanoid  
508 Pigment Produced by Species of the *Sporothrix* Complex in the Presence of L-Tyrosine. *Appl*  
509 *Environ Microbiol* 78: 8623–8630.
- 510 34. EFSA, 2010 (2010) *EFSA J* 8: 1821.
- 511 35. Turick CE, Tisa LS, Frank Caccavo J (2002) Melanin Production and Use as a Soluble Electron  
512 Shuttle for Fe(III) Oxide Reduction and as a Terminal Electron Acceptor by *Shewanella* algae  
513 BrY. *Appl Environ Microbiol* 68: 2436–2444.
- 514 36. Ritz C, Baty F, Streibig JC, et al. (2015) Dose-Response Analysis Using R. *PLoS One* 10: e0146021.
- 515 37. Thompson JD, Gibson TJ, Higgins DG (2002) Multiple sequence alignment using ClustalW and  
516 ClustalX. *Curr Protoc Bioinforma* Chapter 2: Unit 2.3.
- 517 38. Webb B, Sali A (2016) Comparative Protein Structure Modeling Using MODELLER. *Curr Protoc*  
518 *Bioinforma* 54: 5.6.1-5.6.37.
- 519 39. Webb B, Sali A (2017) Protein Structure Modeling with MODELLER, In: Kaufmann M, Klinger C,  
520 Savelsbergh A (Eds.), *Functional Genomics: Methods and Protocols*, New York, NY, Springer, 39–  
521 54.
- 522 40. Yang C, Pflugrath JW, Camper DL, et al. (2004) Structural basis for herbicidal inhibitor selectivity  
523 revealed by comparison of crystal structures of plant and mammalian 4-hydroxyphenylpyruvate  
524 dioxygenases. *Biochemistry* 43: 10414–10423.
- 525 41. Hess B, Kutzner C, van der Spoel D, et al. (2008) GROMACS 4: Algorithms for Highly Efficient,  
526 Load-Balanced, and Scalable Molecular Simulation. *J Chem Theory Comput* 4: 435–447.
- 527 42. Abraham MJ, Murtola T, Schulz R, et al. (2015) GROMACS: High performance molecular  
528 simulations through multi-level parallelism from laptops to supercomputers. *SoftwareX* 1–2:  
529 19–25.
- 530 43. Davis IW, Leaver-Fay A, Chen VB, et al. (2007) MolProbity: all-atom contacts and structure  
531 validation for proteins and nucleic acids. *Nucleic Acids Res* 35: W375–383.
- 532 44. Chen VB, Arendall WB, Headd JJ, et al. (2010) MolProbity: all-atom structure validation for  
533 macromolecular crystallography. *Acta Crystallogr D Biol Crystallogr* 66: 12–21.
- 534 45. Morris GM, Huey R, Lindstrom W, et al. (2009) AutoDock4 and AutoDockTools4: Automated  
535 Docking with Selective Receptor Flexibility. *J Comput Chem* 30: 2785–2791.
- 536 46. Forli S, Huey R, Pique ME, et al. (2016) Computational protein–ligand docking and virtual drug  
537 screening with the AutoDock suite. *Nat Protoc* 11: 905–919.
- 538 47. DeLano WL PyMOL, San Carlos, CA, 700, DeLano Scientifics.
- 539 48. Robin A, Mazurier S, Mougel C, et al. (2007) Diversity of root-associated fluorescent  
540 pseudomonads as affected by ferritin overexpression in tobacco. *Environ Microbiol* 9: 1724–  
541 1737.
- 542 49. Delorme S, Lemanceau P, Christen R, et al. *Pseudomonas lini* sp. nov., a novel species from bulk  
543 and rhizospheric soils. *Int J Syst Evol Microbiol* 52: 513–523.
- 544 50. Piñero S, Rivera J, Romero D, et al. (2007) Tyrosinase from *Rhizobium etli* is involved in  
545 nodulation efficiency and symbiosis-associated stress resistance. *J Mol Microbiol Biotechnol* 13:  
546 35–44.
- 547 51. Tian Y-S, Xu J, Han J, et al. (2013) Complementary screening, identification and application of a  
548 novel class II 5-enopyruvylshikimate-3-phosphate synthase from *Bacillus cereus*. *World J*  
549 *Microbiol Biotechnol* 29: 549–557.

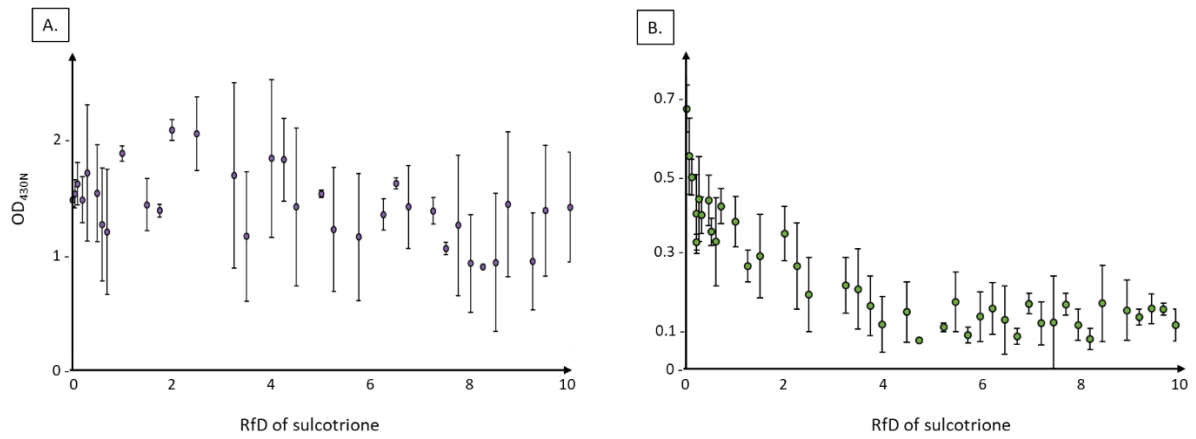
- 550 52. Petric I, Karpouzas DG, Bru D, et al. (2016) Nicosulfuron application in agricultural soils drives  
551 the selection towards NS-tolerant microorganisms harboring various levels of sensitivity to  
552 nicosulfuron. *Environ Sci Pollut Res Int* 23: 4320–4333.
- 553 53. Calvayrac C, Martin-Laurent F, Faveaux A, et al. (2012) Isolation and characterisation of a  
554 bacterial strain degrading the herbicide sulcotrione from an agricultural soil. *Pest Manag Sci* 68:  
555 340–347.
- 556 54. Staub JM, Brand L, Tran M, et al. (2012) Bacterial glyphosate resistance conferred by  
557 overexpression of an E. coli membrane efflux transporter. *J Ind Microbiol Biotechnol* 39: 641–  
558 647.
- 559 55. Li X-Z, Plésiat P, Nikaido H (2015) The challenge of efflux-mediated antibiotic resistance in  
560 Gram-negative bacteria. *Clin Microbiol Rev* 28: 337–418.
- 561 56. Rampioni G, Pillai CR, Longo F, et al. (2017) Effect of efflux pump inhibition on *Pseudomonas*  
562 *aeruginosa* transcriptome and virulence. *Sci Rep* 7.
- 563 57. Ketelboeter LM, Bardy SL (2015) Methods to Inhibit Bacterial Pyomelanin Production and  
564 Determine the Corresponding Increase in Sensitivity to Oxidative Stress. *J Vis Exp JoVE* e53105.
- 565 58. Ketelboeter LM, Bardy SL (2017) Characterization of 2-(2-nitro-4-trifluoromethylbenzoyl)-1,3-  
566 cyclohexanedione resistance in pyomelanogenic *Pseudomonas aeruginosa* DKN343. *PLoS One*  
567 12: e0178084.
- 568 59. Chen W, Wang D, Zhou W, et al. (2016) Novobiocin binding to NaID induces the expression of  
569 the MexAB-OprM pump in *Pseudomonas aeruginosa*. *Mol Microbiol* 100: 749–758.
- 570 60. Hackenberger DK, Stjepanović N, Lončarić Ž, et al. (2018) Acute and subchronic effects of three  
571 herbicides on biomarkers and reproduction in earthworm *Dendrobaena veneta*. *Chemosphere*  
572 208: 722–730.
- 573 61. Dumas E, Giraudo M, Goujon E, et al. (2017) Fate and ecotoxicological impact of new  
574 generation herbicides from the triketone family: An overview to assess the environmental risks.  
575 *J Hazard Mater* 325: 136–156.
- 576 62. Fritze IM, Linden L, Freigang J, et al. (2004) The crystal structures of *Zea mays* and *Arabidopsis*  
577 4-hydroxyphenylpyruvate dioxygenase. *Plant Physiol* 134: 1388–1400.
- 578 63. Pavan ME, Venero ES, Egoburo DE, et al. (2019) Glycerol inhibition of melanin biosynthesis in  
579 the environmental *Aeromonas salmonicida* 34mELT. *Appl Microbiol Biotechnol* 103: 1865–1876.
- 580 64. Bolognese F, Scanferla C, Caruso E, et al. (2019) Bacterial melanin production by heterologous  
581 expression of 4-hydroxyphenylpyruvate dioxygenase from *Pseudomonas aeruginosa*. *Int J Biol*  
582 *Macromol* 133: 1072–1080.
- 583 65. Thiour-Mauprivez C, Devers-Lamrani M, Mounier A, et al. (2020) Design of a degenerate primer  
584 pair to target a bacterial functional community: The hppd bacterial gene coding for the enzyme  
585 targeted by herbicides, a study case. *J Microbiol Methods* 170: 105839.
- 586 66. Moran GR (2014) 4-Hydroxyphenylpyruvate dioxygenase and hydroxymandelate synthase:  
587 Exemplars of the  $\alpha$ -keto acid dependent oxygenases. *Arch Biochem Biophys* 544: 58–68.
- 588 67. Garcia I, Job D, Matringe M (2000) Inhibition of p-Hydroxyphenylpyruvate Dioxygenase by the  
589 Diketetonitrile of Isoxaflutole: A Case of Half-Site Reactivity. *Biochemistry* 39: 7501–7507.
- 590 68. Siehl DL, Tao Y, Albert H, et al. (2014) Broad 4-Hydroxyphenylpyruvate Dioxygenase Inhibitor  
591 Herbicide Tolerance in Soybean with an Optimized Enzyme and Expression Cassette. *Plant*  
592 *Physiol* 166: 1162–1176.
- 593 69. Thiour-Mauprivez C, Martin-Laurent F, Calvayrac C, et al. (2019) Effects of herbicide on non-  
594 target microorganisms: Towards a new class of biomarkers? *Sci Total Environ* 684: 314–325.
- 595 70. Martin-Laurent F, Kandeler E, Petric I, et al. (2013) ECOFUN-MICROBIODIV: an FP7 European  
596 project for developing and evaluating innovative tools for assessing the impact of pesticides on  
597 soil functional microbial diversity--towards new pesticide registration regulation? *Environ Sci*  
598 *Pollut Res Int* 20: 1203–1205.
- 599 71. Karpouzas DG, Tsiamis G, Trevisan M, et al. (2016) 'LOVE TO HATE' pesticides: felicity or curse  
600 for the soil microbial community? An FP7 IAPP Marie Curie project aiming to establish tools for

601 the assessment of the mechanisms controlling the interactions of pesticides with soil  
602 microorganisms. *Environ Sci Pollut Res Int* 23: 18947–18951.

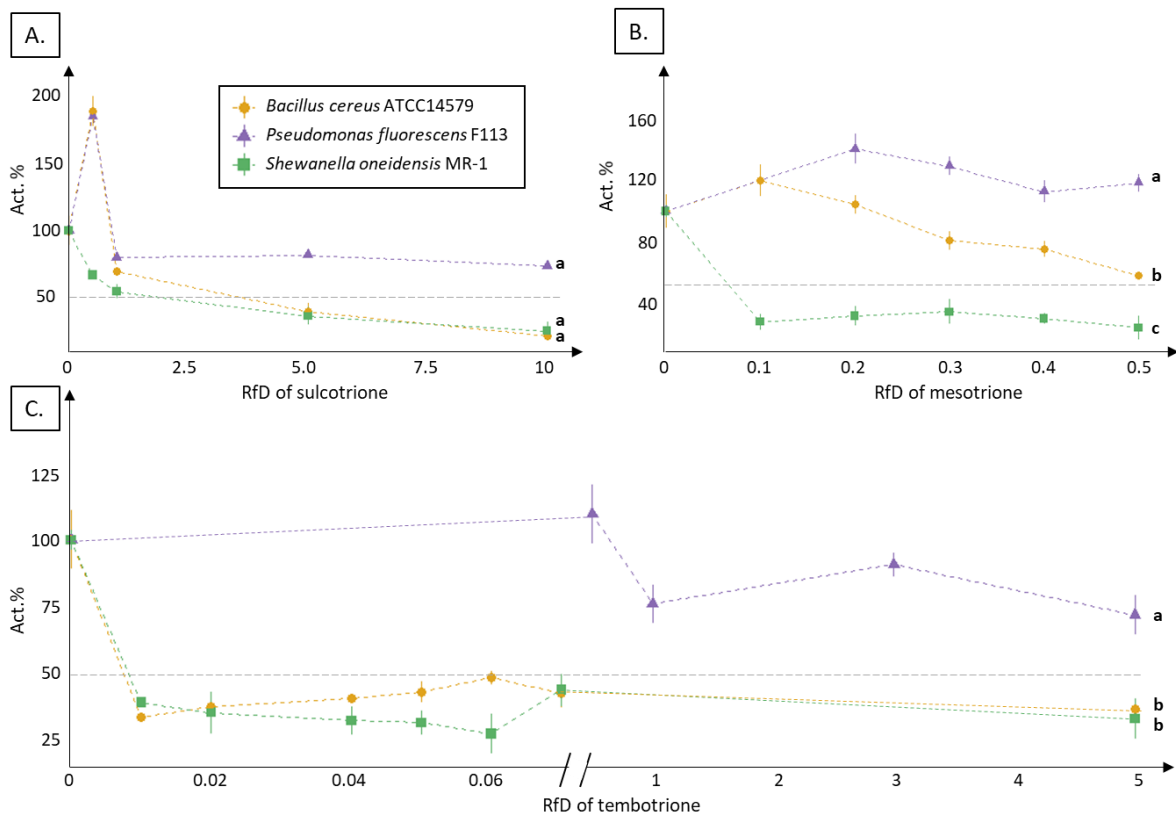
603 **Statements and declarations:** This work was supported by the Région Occitanie and European Funds  
604 for Regional Development (FEDER). Authors also thank Perpignan University Via Domitia for their  
605 financial support (BQR 2018). The authors have no relevant financial or non-financial interests to  
606 disclose. Clémence Thiour-Mauprivez, Lise Barthelmebs, Fabrice Martin-Laurent, Marion Devers-  
607 Lamrani and Christophe Calvayrac conceived and designed research. Franck E. Dayan conducted *in*  
608 *silico* analysis and docking experiments. Clémence Thiour-Mauprivez conducted the resting cells  
609 experiments. Hugo Terol conducted the pyomelanin production measurements. All authors read and  
610 approved the manuscript.



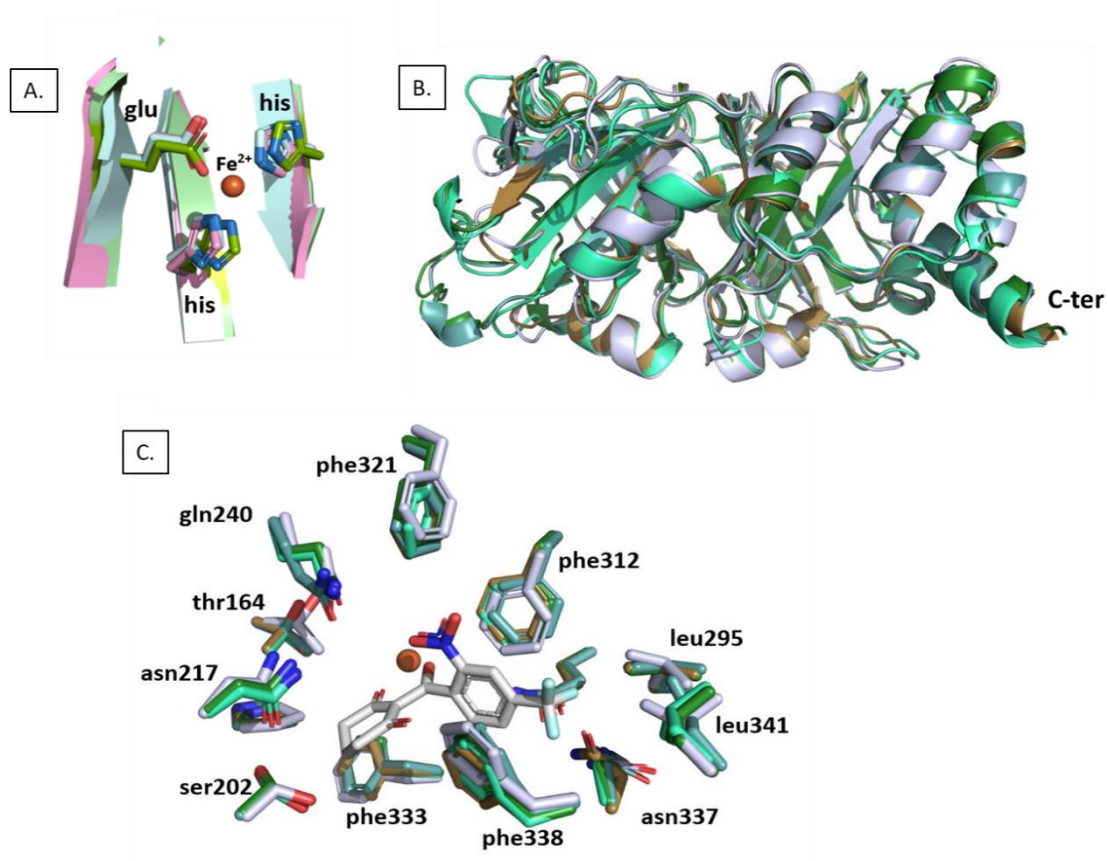
**Figure 1. HPPD relative activity (Act. %) measured in the six different strains (*P. fluorescens* F113, *P. fluorescens* CTR1015 and NEM419, *S. oneidensis* MR-1, *B. cereus* ATCC14579 and *R. etli* CFN42) exposed to 0×, 1× or 10× RfD of sulcotrione. 0× RfD represents the positive control of our experiment. Error bars are calculated from the standard deviation for each series.**



**Figure 2. OD<sub>430N</sub> in *P. fluorescens* F113 (A) and *S. oneidensis* MR-1 (B) in regard to increasing RfD of sulcotrione.** Each value is obtained by subtracting the mean OD<sub>430</sub> obtained at various concentrations of sulcotrione (i.e. OD<sub>430A</sub>) from the mean OD<sub>430</sub> obtained in negative controls (i.e. OD<sub>430NC</sub>) and is depicted on this figure as “OD<sub>430N</sub>”. Error bars are calculated from the standard deviation for each series.

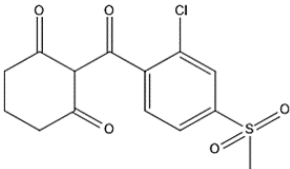
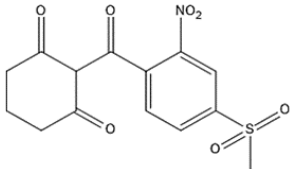
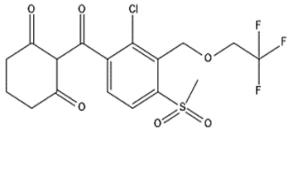


**Figure 3. HPPD relative activity (Act. %) in *B. cereus* ATCC14579, *S. oneidensis* MR-1 and *P. fluorescens* F113 exposed to sulcotrione (A), mesotrione (B) and tembotrione (C).** Act. % represents the percentage obtained by dividing the mean OD<sub>430</sub> obtained at various concentrations of sulcotrione, mesotrione or tembotrione (i.e. OD<sub>430A</sub>) from the mean OD<sub>430</sub> obtained in the positive control (i.e. OD<sub>430PC</sub>). The grey dotted line corresponds to 50% of activity. Error bars are calculated from the standard deviation for each series. **Significant differences between means are indicated by different letters (Kruskal–Wallis tests,  $p < 0.05$ ).**



**Figure 4. A) Residues involved in stabilizing the metal dication ( $\text{Fe}^{2+}$ ) within the HPPD catalytic domain of *P. fluorescens* in pink (1cxj), *A. thaliana* in green (6isd) and *H. sapiens* in blue (3isq). B) Alignment of the 4 bacterial models derived from the HPPD sequences of *P. fluorescens* F113, *B. cereus* ATCC14579, *S. oneidensis* MR-1 and *R. etli* CFN42. C) Amino acid residues lining the substrate binding pocket of HPPD are highly conserved of the 4 bacterial homology models. Numbering is based on sequence of *P. fluorescens* HPPD.**

**Table 1.  $\beta$ -triketone molecules used as herbicides.** CMBA: 2-chloro-4-methyl sulfonyl benzoic acid; CHD: 1,3-cyclohexanedione MNBA: 4-methylsulfonyl-2-nitro benzoic acid; AMBA: 2-amino-4-methylsulfonylbenzoic acid TCMBA: 2-(2-chloro-4-mesyl-3-(2,2,2-trifluoroethoxy) methyl) benzoic acid.

Molecule	Sulcotrione	Mesotrione	Tembotrione
Chemical structure			
IUPAC name	2-(2-Chloro-4-(methylsulfonyl)benzoyl)cyclohexane-1,3-dione	2-(4-mesyl-2-nitrobenzoyl)cyclohexane-1,3-dione	2-(2-Chloro-4-((2,2,2-trifluoroethoxy)methyl)benzoyl)cyclohexane-1,3-dione
MW (g/mol)	324.8	339.3	440.8
pKa	3.13	3.12	3.18
Solubility in water at pH 7 (g/L)	0.17	15	28.3
Log Kow	0.55	-0.17	1.8
Main degradation product	CMBA; CHD	MNBA; AMBA	TCMBA